Journal of Virology

Virology | Full-Length Text

The Ca^{2+}-dependent phosphatase calcineurin dephosphorylates TBK1 to suppress antiviral innate immunity

Yang Qu,[1,2] Siyuan Wang,[2,3] Hui Jiang,[2] Qingyi Wang,[2,3] Ying Liao,[2] Xusheng Qiu,[2] Lei Tan,[2] Cuiping Song,[2] Chan Ding,[2,4] Yingjie Sun,[2] Zengqi Yang[1]

AUTHOR AFFILIATIONS See affiliation list on p. 18.

ABSTRACT Tumor necrosis factor receptor-associated factor family member-associated NF-κB activator-binding kinase 1 (TBK1) plays a key role in the induction of the type 1 interferon (IFN-I) response, which is an important component of innate antiviral defense. Viruses target calcium (Ca^{2+}) signaling networks, which participate in the regulation of the viral life cycle, as well as mediate the host antiviral response. Although many studies have focused on the role of Ca^{2+} signaling in the regulation of IFN-I, the relationship between Ca^{2+} and TBK1 in different infection models requires further elucidation. Here, we examined the effects of the Newcastle disease virus (NDV)-induced increase in intracellular Ca^{2+} levels on the suppression of host antiviral responses. We demonstrated that intracellular Ca^{2+} increased significantly during NDV infection, leading to impaired IFN-I production and antiviral immunity through the activation of calcineurin (CaN). Depletion of Ca^{2+} was found to lead to a significant increase in virus-induced IFN-I production resulting in the inhibition of viral replication. Mechanistically, the accumulation of Ca^{2+} in response to viral infection increases the phosphatase activity of CaN, which in turn dephosphorylates and inactivates TBK1 in a Ca^{2+}-dependent manner. Furthermore, the inhibition of CaN on viral replication was counteracted in *TBK1* knockout cells. Together, our data demonstrate that NDV hijacks Ca^{2+} signaling networks to negatively regulate innate immunity via the CaN-TBK1 signaling axis. Thus, our findings not only identify the mechanism by which viruses exploit Ca^{2+} signaling to evade the host antiviral response but also, more importantly, highlight the potential role of Ca^{2+} homeostasis in the viral innate immune response.

IMPORTANCE Viral infections disrupt intracellular Ca^{2+} homeostasis, which affects the regulation of various host processes to create conditions that are conducive for their own proliferation, including the host immune response. The mechanism by which viruses trigger TBK1 activation and IFN-I induction through viral pathogen-associated molecular patterns has been well defined. However, the effects of virus-mediated Ca^{2+} imbalance on the IFN-I pathway requires further elucidation, especially with respect to TBK1 activation. Herein, we report that NDV infection causes an increase in intracellular free Ca^{2+} that leads to activation of the serine/threonine phosphatase CaN, which subsequently dephosphorylates TBK1 and negatively regulates IFN-I production. Furthermore, depletion of Ca^{2+} or inhibition of CaN activity exerts antiviral effects by promoting the production of IFN-I and inhibiting viral replication. Thus, our results reveal the potential role of Ca^{2+} in the innate immune response to viruses and provide a theoretical reference for the treatment of viral infectious diseases.

KEYWORDS Ca^{2+}, virus infection, calcineurin, TBK1, antiviral immunity

As the first defense against viral infection, the innate immune system senses the invasion of pathogens through several pattern recognition receptors (PRRs),

Editor Martin Schwemmle, University Medical Center Freiburg, Freiburg, Germany

Address correspondence to Chan Ding, shoveldeen@shvri.ac.cn, Yingjie Sun, sunyingjie@shvri.ac.cn, or Zengqi Yang, yzq8162@163.com.

The authors declare no conflict of interest.

See the funding table on p. 18.

Received 6 February 2024
Accepted 6 March 2024
Published 2 April 2024

including toll-like receptors (TLRs), retinoic acid-inducible gene I-like receptors (RLRs), cytosolic DNA sensors, and nucleotide-binding oligomerization domain-like receptors (NLRs), which initiate a series of signaling events to induce interferons (IFNs) and other inflammatory cytokines to protect host cells (1). Tumor necrosis factor receptor-associated factor family member-associated NF-κB activator-binding kinase 1 (*TBK1*) is an immune evasion gene and a key factor in the antiviral innate immune response (2). Activated TBK1 induces the phosphorylation of interferon regulatory factor 3 (IRF3) and its translocation to the nucleus, thereby initiating IFN-β expression. Multiple post-translational modifications, including phosphorylation, ubiquitination, SUMOylation, and acetylation, are involved in the regulation of TBK1 activity and stability (3–7). TBK1 modifications are tightly and precisely regulated by protein kinases or ubiquitin ligases. However, few studies have examined the role of second messengers such as calcium (Ca^{2+}) on the regulation of TBK1 activity.

As a ubiquitous intracellular second messenger, Ca^{2+} is involved in the regulation of a broad range of cellular processes, including cell growth and proliferation, energy metabolism, and signal transduction (8). Intracellular Ca^{2+} homeostasis is an important prerequisite for maintaining the normal life cycle of a cell. An imbalance in Ca^{2+} can lead to the disruption of some Ca^{2+}-dependent enzymatic processes, alter the expression of Ca^{2+}-sensitive transcriptional factors, or inactivate Ca^{2+}-dependent proteins, thereby disrupting the integrity of cellular structure and function (9–11). Thus, viruses often target Ca^{2+} signaling pathways to create conditions that are conducive to the replication of progeny viruses (12). Viral proteins directly or indirectly disrupt intracellular Ca^{2+} homeostasis by modulating Ca^{2+} channels and pumps or host membrane permeability, which causes stress on Ca^{2+} storage organelles, such as the endoplasmic reticulum (ER) or mitochondria (13, 14). For example, the human immunodeficiency virus (HIV) accessory protein Nef cooperates with Vpr to trigger the release of ER Ca^{2+} (15), while hepatitis C virus (HCV) promotes Ca^{2+} uptake in mitochondria, leading to mitochondrial stress injury and the production of reactive oxygen species (16). In response to viral invasion, host cells exploit Ca^{2+} signaling networks to regulate the activation of PRR-triggered innate immunity and inflammatory responses (17). For example, upon viral infection, high Ca^{2+} has been shown to upregulate the mRNA expression of TLRs (such as TLR3) and RLRs (such as MDA5 and RIG-I) to enhance antiviral activity (18). In addition, some viruses promote Ca^{2+} flux, which then triggers the formation and activation of NLRs, such as the NLRP3 inflammasome (19, 20). The cytosolic DNA sensor complex, cyclic GMP-AMP synthase-stimulator of interferon (STING), has also been shown to be regulated by Ca^{2+} and related signaling proteins (21). However, few studies have focused on the role of Ca^{2+} in the regulation of signaling transduction molecules, such as TBK1 and IRF3.

Calcineurin (CaN) is a highly conserved serine/threonine phosphatase present in eukaryotes that is primarily located in the cytosol and is involved in a variety of signaling processes (22, 23). CaN directly links Ca^{2+} signaling to the protein phosphorylation state of various substrates, thus playing an important role in numerous signal transduction processes (24). CaN is activated by the Ca^{2+}-sensing protein calmodulin (CaM) in response to increased intracellular Ca^{2+} concentrations. CaM is a small, highly conserved, ubiquitously expressed calcium-binding protein that possesses no enzymatic activity and is absolutely dependent on Ca^{2+} (25). At high Ca^{2+} concentrations, both CaN and CaM bind to Ca^{2+} to form a CaM-CaN complex which promotes CaN phosphatase activity and directly links Ca^{2+} signaling to the dephosphorylation of substrates (25, 26). Currently, the most extensively studied substrates of CaN are transcription factors, such as nuclear factor of activated T-cells (27, 28), forkhead transcription factors (29), myocyte-specific enhancer factor 2 (30), and transcription factor EB (TFEB) (31). CaN is also involved in regulating the activity of several receptors and ion channels, thereby controlling a variety of signaling pathways (23, 32, 33). In addition, CaN is thought to interact with mitochondria-associated proteins to regulate mitochondrial dynamics or structural integrity (34). For example, CaN has been shown to dephosphorylate dynamin-related protein 1, thereby promoting mitochondrial fission (35). In recent years, the

molecular structure, enzymatic characteristics, and biological functions of CaN have been extensively studied, and the results have been gradually applied to the treatment of organ transplant rejection and cardiovascular and cerebrovascular diseases (22, 30, 36). However, the role of CaN in viral infectious diseases is poorly understood.

Newcastle disease virus (NDV) is a highly contagious avian pathogen of the Paramyxoviridae family. Diseases caused by NDV can cause significant economic losses (37). NDV is also known to be an oncolytic virus that can replicate selectively in host and tumor cells, thereby inducing ER stress and altering mitochondrial dynamics (38, 39), which are important inducers of intracellular Ca^{2+} homeostasis. Our preliminary results showed that NDV infection led to increased accumulation of intracellular Ca^{2+}, while inhibition of this NDV-mediated increase in Ca^{2+} inhibited viral replication and activated the innate immune response. Here, we further demonstrate that NDV infection restricts TBK1 signaling and type 1 interferon (IFN-I) expression in a CaN-dependent manner through the induction of intracellular Ca^{2+} accumulation, thereby allowing the virus to escape the immune response and promote its own replication and proliferation. In summary, our findings demonstrate that NDV uses CaN to fight the innate immune response. Furthermore, we provide molecular insights into the host antiviral effects through the maintenance of Ca^{2+} homeostasis.

RESULTS

NDV infection promotes intracellular Ca^{2+} accumulation

Since Ca^{2+} is an important ubiquitous second messenger in cells, some viral infections will inevitably cause its homeostatic imbalance (12). The ER is the largest intracellular Ca^{2+} reservoir, and ER stress induced by NDV infection may therefore induce an imbalance in Ca^{2+} homeostasis. Thus, we first asked whether NDV infection disrupted Ca^{2+} homeostasis to promote its own replication. Using Fluo-4 AM labeling to detect intracellular Ca^{2+} levels during NDV infection, we found that NDV infection led to the significant accumulation of intracellular Ca^{2+} in a time- and dose-dependent manner, characterized by an increased number of positive fluorescent cells (Fig. 1A through C) and Fluo-4 AM fluorescence intensity (Fig. 1D through F). In the attenuated NDV LaSota infection model expressing red fluorescent protein (RFP-LaSota), it was observed that the accumulation of intracellular Ca^{2+} specifically occurred in the infected cells due to viral infection, rather than in uninfected bystander cells (Fig. 1G and H). Treatment with 2-aminoethoxydiphenyl borate (2-APB), which inhibits D-myo-inositol 1,4,5-trisphosphate receptor (IP_3R) to prevent Ca^{2+} release from the ER, or the intracellular Ca^{2+} chelator 1,2-bis(2-aminophenoxy)ethane-N,N,N′,N′-tetraacetic acid tetrakis(acetoxymethyl ester) (BAPTA-AM) was found to significantly reverse the NDV-induced accumulation of cytoplasmic free Ca^{2+} (Fig. 1I and J) without affecting cell viability (Fig. 2A and B). Together, these results demonstrate that NDV infection induces intracellular Ca^{2+} accumulation by stimulating ER Ca^{2+} release and extracellular Ca^{2+} influx.

Inhibition of ER Ca^{2+} release broadly inhibits viral proliferation

Since significant accumulation of intracellular Ca^{2+} was observed during NDV infection, we next sought to determine the effects of Ca^{2+} accumulation on viral replication in A549 cells. We found that NDV viral nucleoprotein (NP) levels were markedly reduced in a dose-dependent manner after ER Ca^{2+} release was blocked by 2-APB (Fig. 2C). Interestingly, chelation of intracellular Ca^{2+} following BAPTA-AM treatment had no obvious effects on NDV replication (Fig. 2D). The inhibitory effects of 2-APB on different stages of NDV infection were examined further by evaluating viral gene transcription, protein synthesis, and extracellular viral yields at different time points post-infection (pi). We found that treatment with 2-APB significantly reduced the expression of Newcastle disease virus nucleoprotein (NDV-NP) at both mRNA and protein levels at 6, 12, 18, and 24 h pi (Fig. 2E and F). Similarly, treatment with 2-APB decreased the extracellular viral titer in the cell supernatant as measured by $TCID_{50}$ and the plaque assay (Fig. 2G and H).

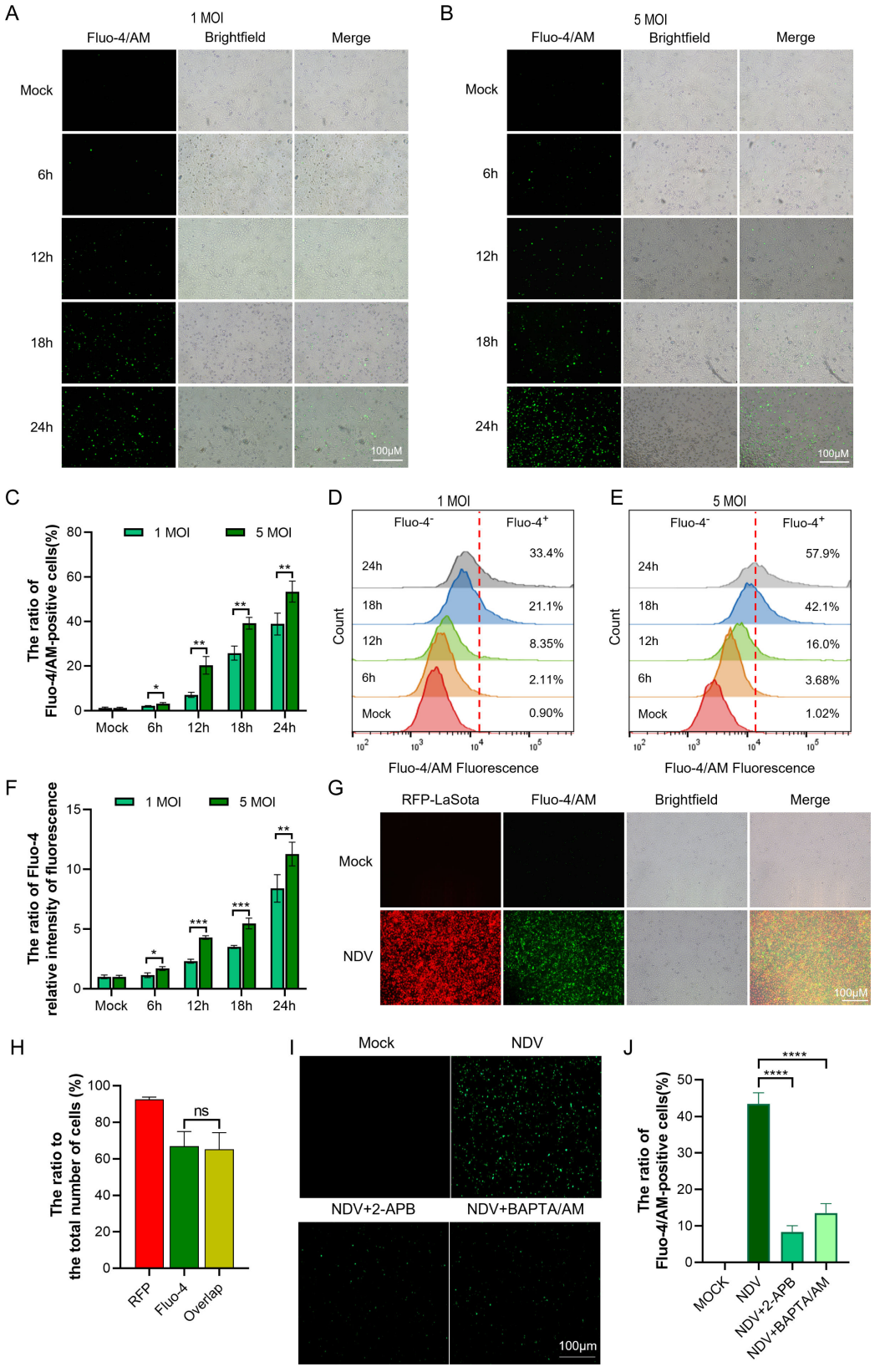

FIG 1 NDV infection promotes intracellular Ca^{2+} accumulation. A549 cells were infected with NDV at an MOI of 1 or 5. Cells were harvested at 0, 6, 12, 18, and 24 h post-infection, then incubated with the fluorescent calcium indicator, Fluo-4/AM. (A and B) Ca^{2+} concentrations in the cytosol were visualized by fluorescence microscopy. (C) Quantification of the free

(Continued on next page)

FIG 1 (Continued)

Ca^{2+} levels in the cytosol by the number of positive fluorescent cells. (D and E) Fluorescence intensity was detected by flow cytometry. (F) Quantification of the free Ca^{2+} levels in the cytosol by fluorescence intensity. (G) Attenuated NDV strain RFP-LaSota-infected A549 cells for 24 h and then labeled with Fluo-4/AM for free Ca^{2+}. (H) Quantification of overlapping red and green fluorescence. (I) A549 cells were treated with 2-APB (100 µM) and BAPTA-AM (20 µM), then infected with NDV for 18 h, and incubated with Fluo-4/AM. Ca^{2+} concentrations in the cytosol were visualized by fluorescence microscopy. (J) Quantitation of the free Ca^{2+} levels in the cytosol. Each bar represents the mean ± standard deviation. *$P < 0.05$, **$P < 0.01$, ***$P < 0.001$, ****$P < 0.0001$. MOI, multiplicity of infection; ns, not significant.

The antiviral effects of 2-APB were next examined using an attenuated NDV LaSota strain expressing green fluorescent protein (GFP-LaSota). 2-APB treatment was found to also suppress attenuated GFP-LaSota proliferation (Fig. 2I). To eliminate any off-target effects of the inhibitor 2-APB, we also used small interfering RNA (siRNA) to knock down the ER Ca^{2+} release channel IP_3R_1. The results showed that knockdown IP_3R_1 also inhibited the replication of NDV (Fig. 2J through L). Similar antiviral effects of 2-APB or knockdown IP_3R_1 were observed in infection models with Sendai virus (SeV), avian influenza virus (AIV), vesicular stomatitis virus (VSV), and herpes simplex virus-1 (HSV-1) (Fig. S1A and B). These results were further replicated in H1299 cells, DF-1 cells, and chicken embryo fibroblast (CEF) cells (Fig. S2). Together, our findings demonstrate that blocking ER Ca^{2+} release inhibits viral proliferation.

Depletion of extracellular Ca^{2+} suppresses viral proliferation

The influx of extracellular Ca^{2+} is important for the maintenance of Ca^{2+} homeostasis. Thus, we used a Ca^{2+}-free medium to deplete extracellular Ca^{2+} to determine whether the absence of extracellular Ca^{2+} had a similar inhibitory effect on viral replication. We first confirmed that the absence of Ca^{2+} in the culture medium had no significant impact on cell viability (Fig. 3A). Next, we demonstrated that a deficiency in extracellular Ca^{2+} greatly impeded the replication of NDV, as measured by a decrease in viral mRNA (Fig. 3B) and protein levels (Fig. 3C), together with a reduction in viral titers in the cell supernatant (Fig. 3D and E). Similar results were obtained in the GFP-LaSota infection model (Fig. 3F), as well as in the four following viruses: SeV, AIV, VSV, and HSV-1 (Fig. S1C). Our findings were also replicated identically in H1299, CEF, and DF-1 cells (Fig. S3). The effects of extracellular Ca^{2+} on viral replication were determined by adding $CaCl_2$ to the culture medium. Addition of $CaCl_2$ only had a minor positive effect on viral replication, suggesting the extra Ca^{2+} had a limited role in viral replication (Fig. 3G). Collectively, our results indicate that similar to the antiviral effects induced by blockage of ER Ca^{2+} release, depletion of extracellular Ca^{2+} also inhibits viral replication and proliferation.

Inhibition of ER Ca^{2+} release, but not depletion of extracellular Ca^{2+}, promotes activation of the IFN-β signaling pathway

The IFN-mediated innate immune response is one of the most important antiviral responses at the cellular level, and although the mechanism has not been fully elucidated, Ca^{2+} has been shown to play a role (12, 17). Here, we speculated that inhibition of Ca^{2+} flux exerts its antiviral effects through regulation of the innate immune response. First, we detected components of the IFN-β signaling pathway in NDV-infected A549 cells treated with 2-APB. We found that 2-APB treatment led to an increase in IFN-β and ISG (IFIT-1 and MX1) mRNA levels after NDV infection (Fig. 4A). Similar results were obtained in cells treated with the TLR3 agonist polyinosinic-polycytidylic acid [poly(I:C)] (Fig. 4B). In addition, we found that NDV-induced phosphorylation of TBK1 (Ser172) and transcription factor IRF3 (Ser396), which are responsible for initiating the production of IFN-I, was significantly enhanced in 2-APB-treated A549 cells (Fig. 4C). Furthermore, 2-APB treatment also increased the nuclear translocation of IRF3 after NDV infection (Fig. 4D). Similarly, IP_3R_1 knockdown led to an increase in IFN-β and ISGs (IFIT-1 and MX1) mRNA levels (Fig. 4E) and promoted the phosphorylation of TBK1 and IRF3

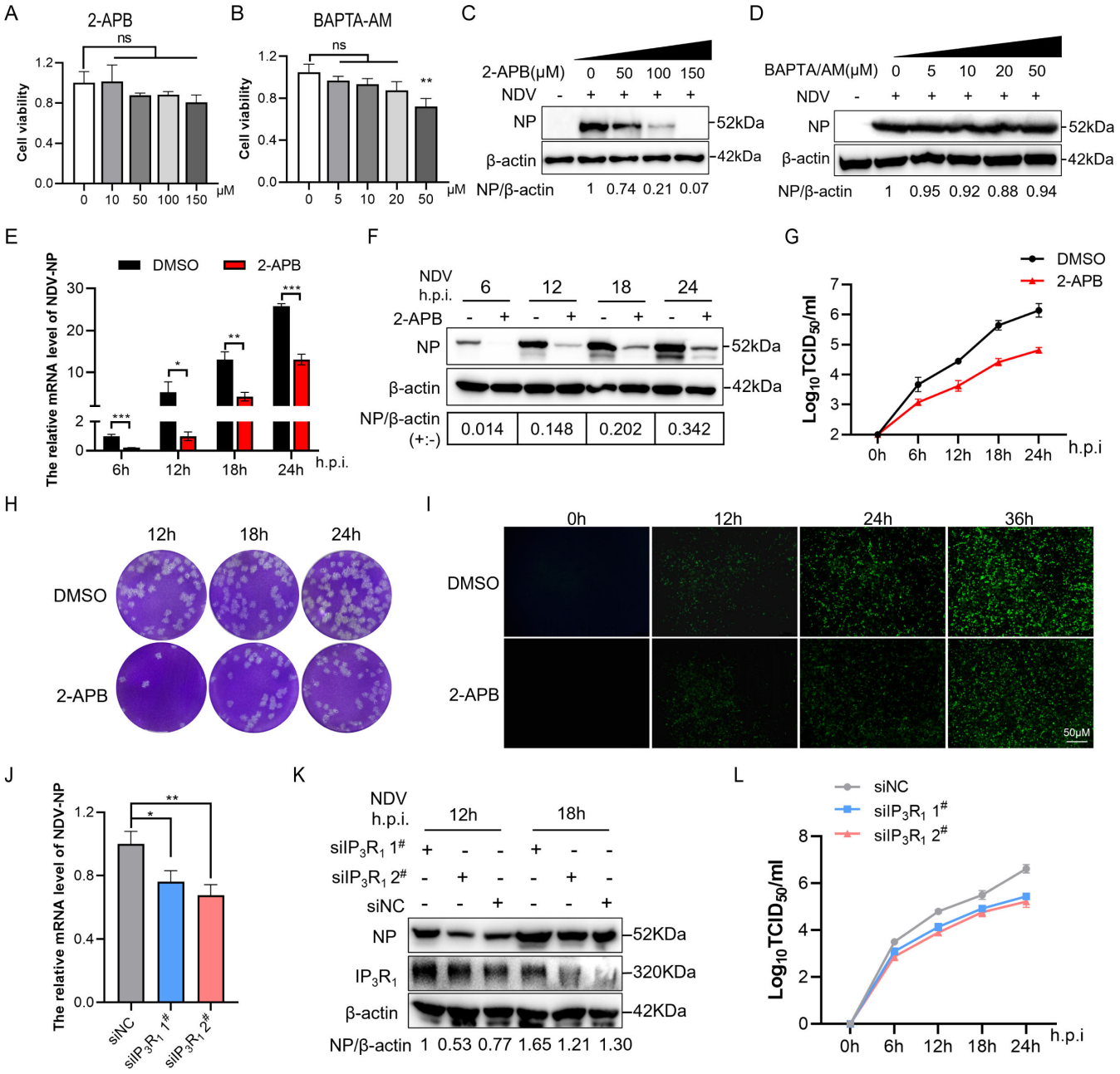

FIG 2 Inhibition of ER Ca^{2+} release inhibits viral proliferation. (A and B) A549 cells were spread on a 96-well plate for 24 h, and the effects of different inhibitor concentrations on cell viability were detected by CCK-8. (C) A549 cells were treated with 2-APB (0, 50, 100, and 150 μM), then infected with NDV at an MOI of 1. Cells were harvested at 18 h post-infection. Western blot analysis was used to assess NDV-NP protein expression levels. β-Actin acted as the loading control. (D) A549 cells were treated with BAPTA-AM (0, 5, 10, 20, and 50 μM), then infected with NDV at an MOI of 1. Cells were harvested at 18 h post-infection. Western blot analysis was used to assess NDV-NP expression levels. β-Actin acted as the loading control. (E–H) A549 cells were treated with or without 2-APB (100 μM), then mock treated or infected with NDV at an MOI of 1. Cells were harvested at 0, 6, 12, 18, and 24 h post-infection. The amounts of viral mRNA (E) and protein (F) were assessed in the cell lysates, while cell culture supernatants were subjected to the viral titer assay (G), and the virus yield was analyzed by plaque assays (H). (I) A549 cells were treated with or without 2-APB (100 μM) followed by infection with the attenuated NDV strain GFP-LaSota. Viral proliferation was visualized 0, 12, 24, and 36 h post-infection by fluorescence microscopy. (J–L) A549 cells were transfected with IP_3R_1 small interfering RNA for 48 h, then infected with NDV at an MOI of 1. At 12 h post-infection, cells were harvested, and quantitative real-time PCR was used to assess NDV-NP mRNA expression levels (J). At 12 or 18 h post-infection, NDV-NP expression levels were assessed by Western blotting (K). Cell culture supernatants were then subjected to the viral titer assay (L). Each bar represents the mean ± standard deviation. *$P < 0.05$, **$P < 0.01$, ***$P < 0.001$. DMSO, dimethyl sulfoxide; NDV-NP, Newcastle disease virus nucleoprotein; NP, nucleoprotein.

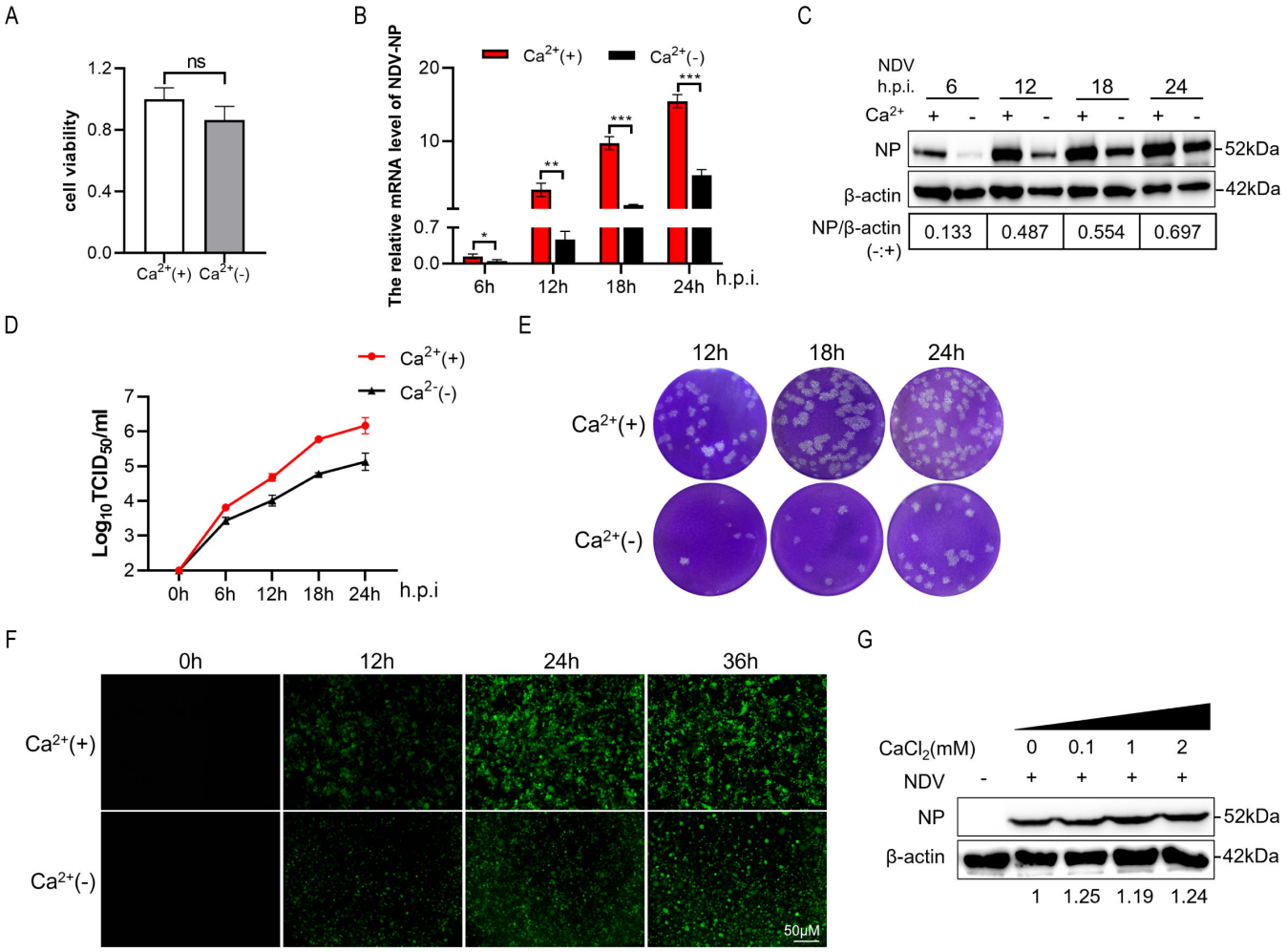

FIG 3 Depletion of extracellular Ca^{2+} suppresses viral proliferation. (A) Cells were cultured with Ca^{2+}-free medium for 24 h, and then cell viability was measured by CCK-8. (B–E) A549 cells were cultured in normal medium or calcium-free medium followed by infection with NDV at an MOI of 1 for 0, 6, 12, 18, and 24 h. The amount of viral mRNA (B) and protein (C) was assessed in the cell lysates, while cell culture supernatants were subjected to the viral titer assay (D), and the virus yield was analyzed by plaque assays (E). (F) Attenuated NDV strain GFP-LaSota-infected A549 cells were cultured in normal or calcium-free medium. Viral proliferation was visualized by fluorescence microscopy. (G) A549 cells were treated with $CaCl_2$ (0, 0.1, 1.0, and 2.0 mM), then infected with NDV for 18 h. Western blot analysis was used to examine the expression levels of NDV-NP. β-Actin acted as the loading control. Each bar represents the mean ± standard deviation. *P < 0.05, **P < 0.01, ***P < 0.001.

after NDV infection (Fig. 4F). These findings demonstrated that treatment with 2-APB or knockdown IP_3R_1 promotes IFN-I production to achieve antiviral effects. Unexpectedly, we also found that, although the absence of extracellular Ca^{2+} also significantly inhibited viral replication, it had no positive effect on IFN-I production but rather suppressed IFN-β and ISGs mRNA levels, probably due to lower viral replication efficiency after depletion of extracellular Ca^{2+} (Fig. 4G). Accordingly, NDV-induced phosphorylation of both TBK1 and IRF3 was lower in the absence of Ca^{2+} (Fig. 4H). These results indicate that inhibition of ER Ca^{2+} release, but not depletion of extracellular Ca^{2+}, activates the IFN-I signaling pathway.

NDV infection activates CaN to negatively regulate IFN-I signaling

Since blocking the release of ER Ca^{2+} was found to promote IFN-I production and because CaN is a Ca^{2+}-dependent phosphatase, we speculated that NDV infection restricts IFN-I production by regulating the activity of CaN. Treatment with cyclosporin A (CsA), an inhibitor of the phosphatase activity of CaN, led to an increase in NDV-induced IFN-β, IFIT-1, and MX1 production (Fig. 5A) without affecting cell viability (Fig. 6A).

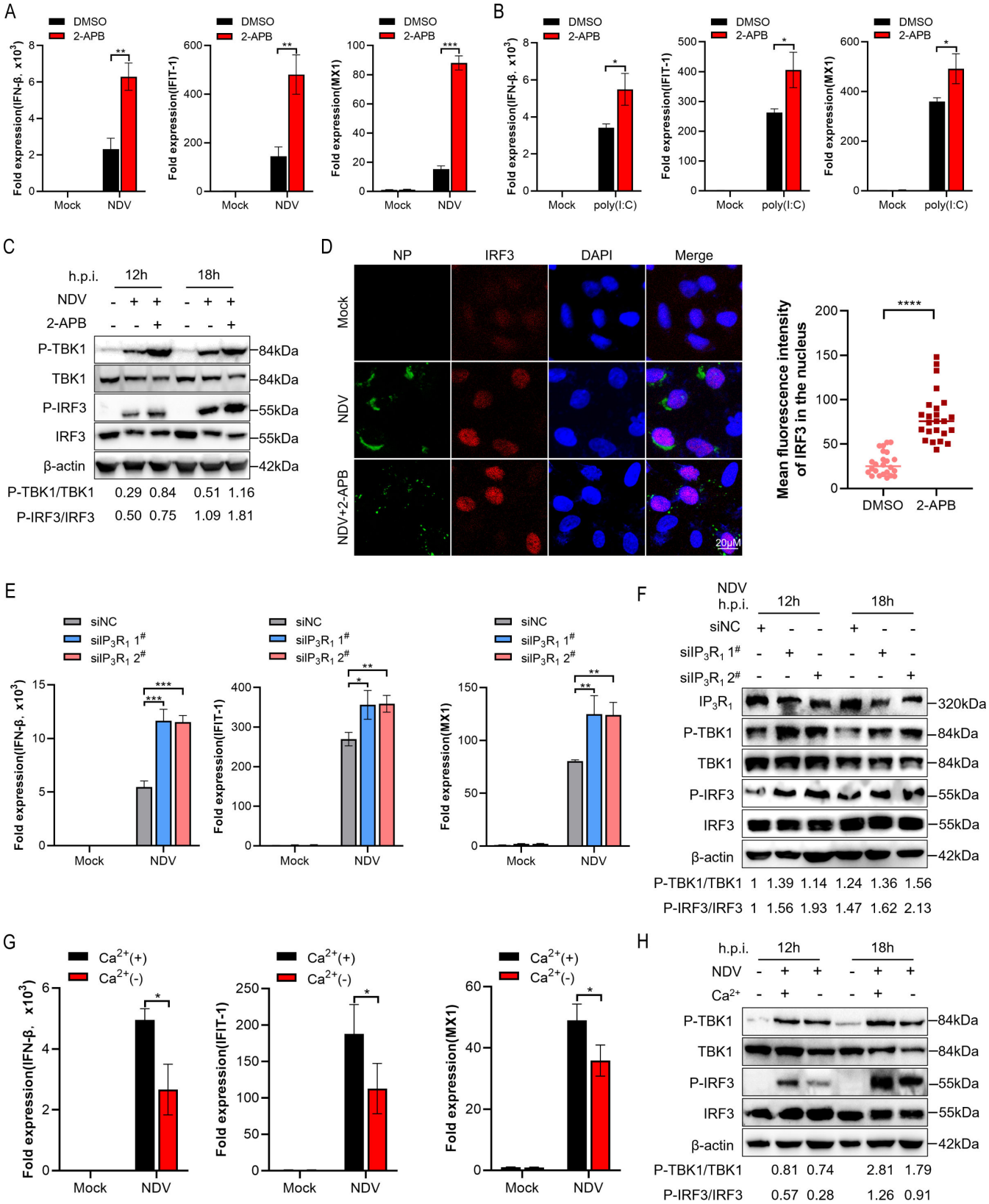

FIG 4 Inhibition of ER Ca^{2+} release promotes activation of the IFN-β signaling pathway. (A) A549 cells were treated with or without 2-APB (100 μM), then mock treated or infected with NDV at an MOI of 1. At 12 h post-infection, cells were harvested, and qRT-PCR was used to assess IFN-β, IFIT-1, and MX1 mRNA expression levels. (B) A549 cells were treated with or without 2-APB (100 μM), then mock treated or transfected with poly(I:C) (20 mg/mL). Cells were harvested after 12 h,

(Continued on next page)

FIG 4 (Continued)

and qRT-PCR was used to examine IFN-β, IFIT-1, and MX1 mRNA expression levels. (C) Virus infection experiments were performed as described above for panel A. Cells were harvested at 12 and 18 h post-infection, and P-TBK1, TBK1, P-IRF3, and IRF3 protein expression levels were assessed by Western blot analysis. β-Actin acted as the loading control. (D) Virus infection experiments were performed as described above for panel A. At 18 h post-infection, cells were fixed and immunofluorescence staining was carried out using antibodies against IRF3 and NDV-NP. Nuclei were stained with 1-mg/mL 4′,6-diamidino-2-phenylindole (DAPI). (E and F) A549 cells were transfected with IP_3R_1 siRNA for 48 h, then infected with NDV at an MOI of 1. At 12 h post-infection, cells were harvested, and qRT-PCR was used to examine IFN-β, IFIT-1, and MX1 mRNA expression levels (E). At 12 or 18 h post-infection, P-TBK1, TBK1, P-IRF3, and IRF3 protein expression levels were assessed by Western blot analysis (F). (G) A549 cells were cultured in normal medium or calcium-free medium, then mock treated or infected with NDV at an MOI of 1. At 12 h post-infection, cells were harvested, and qRT-PCR was used to detect IFN-β, IFIT-1, and MX1 mRNA expression levels. (H) Virus infection experiments were performed as described above for panel G. Cells were harvested at 12 and 18 h post-infection, and P-TBK1, TBK1, P-IRF3, and IRF3 protein expression levels were measured by Western blotting. β-Actin acted as the loading control. Each bar represents the mean ± standard deviation. *$P < 0.05$, **$P < 0.01$, ***$P < 0.001$, ****$P < 0.0001$. qRT-PCR, quantitative real-time PCR.

Similarly, treatment with CsA significantly increased NDV-induced phosphorylation of both TBK1 and IRF3 (Fig. 5B). Next, we used siRNAs to construct targeting the CaN knockdown cells (Fig. 5C). We found that CaN knockdown led to an increase in IFN-β and ISG (IFIT-1 and MX1) mRNA levels (Fig. 5D). Furthermore, knockdown of CaN also promoted TBK1 and IRF3 phosphorylation after NDV infection (Fig. 5E), suggesting that CaN negatively regulates NDV-induced IFN-I production.

Previous studies have shown that CaN deactivates TBK1 through dephosphorylation (40). To further elucidate the mechanism by which NDV-induced CaN blocks IFN-I production, we next asked whether CaN binds to TBK1 during NDV infection. We confirmed that there was an interaction between CaN and TBK1 (Fig. 5F) and that NDV infection increased this interaction (Fig. 5G). In addition, we showed that CaN activity gradually increased during the middle stages of viral infection, especially at 12 and 18 h post-NDV infection (Fig. 5I). However, NDV infection did not lead to an increase in CaN protein expression levels (Fig. 5H). In addition, 2-APB effectively inhibited the NDV-induced elevation of CaN activity (Fig. 5J), suggesting that the increase in CaN activity coincided with the virus-induced elevation in intracellular Ca^{2+} levels (Fig. 1I). Together, our results indicate that NDV infection activates CaN in a Ca^{2+}-dependent manner, leading to the subsequent dephosphorylation and inhibition of TBK1.

Inhibition of CaN activity inhibits viral replication

To further confirm the role of CaN activity in viral proliferation, we next examined the effects of CaN inhibition or knockdown on NDV replication. We found that CsA inhibited NDV replication in a dose-dependent manner (Fig. 6B). Treatment with CsA reduced the expression of NDV-NP at both the mRNA and protein levels (Fig. 6C and D), as well as decreased the extracellular viral titer (Fig. 6E). At the same time, we found that NDV replication was significantly decreased in CaN knockdown cells (Fig. 6F through H). Similarly, both CsA treatment and knockdown of CaN inhibited viral replication in other viral infection models, including SeV, AIV, VSV, and HSV (Fig. S4). Together, these results suggest that inhibition of CaN activity or knockdown of CaN can inhibit viral proliferation.

Knockout of *TBK1* inhibits the effect of Ca^{2+} and CaN on viral proliferation

To further emphasize the bridging role of TBK1 in Ca^{2+}-regulated viral replication, the effect of Ca^{2+} and CaN on virus proliferation was examined in *TBK1* knockout (*TBK1*$^{-/-}$) cells. Compared with the significant inhibition of NDV proliferation by 2-APB treatment in wild-type (WT) cells, no inhibitory effect was observed in *TBK1*$^{-/-}$ cells, as evidenced by the expression of NDV-NP at both mRNA and protein levels (Fig. 7A and B), and the extracellular viral titer in the cell supernatant (Fig. 7C), respectively. Interestingly, we cultured *TBK1*$^{-/-}$ cells using Ca^{2+}-free media, in which NDV proliferation was still significantly inhibited (Fig. 7D through F), indicating that the function of extracellular Ca^{2+} on NDV proliferation does not depend on the presence of TBK1. This is consistent

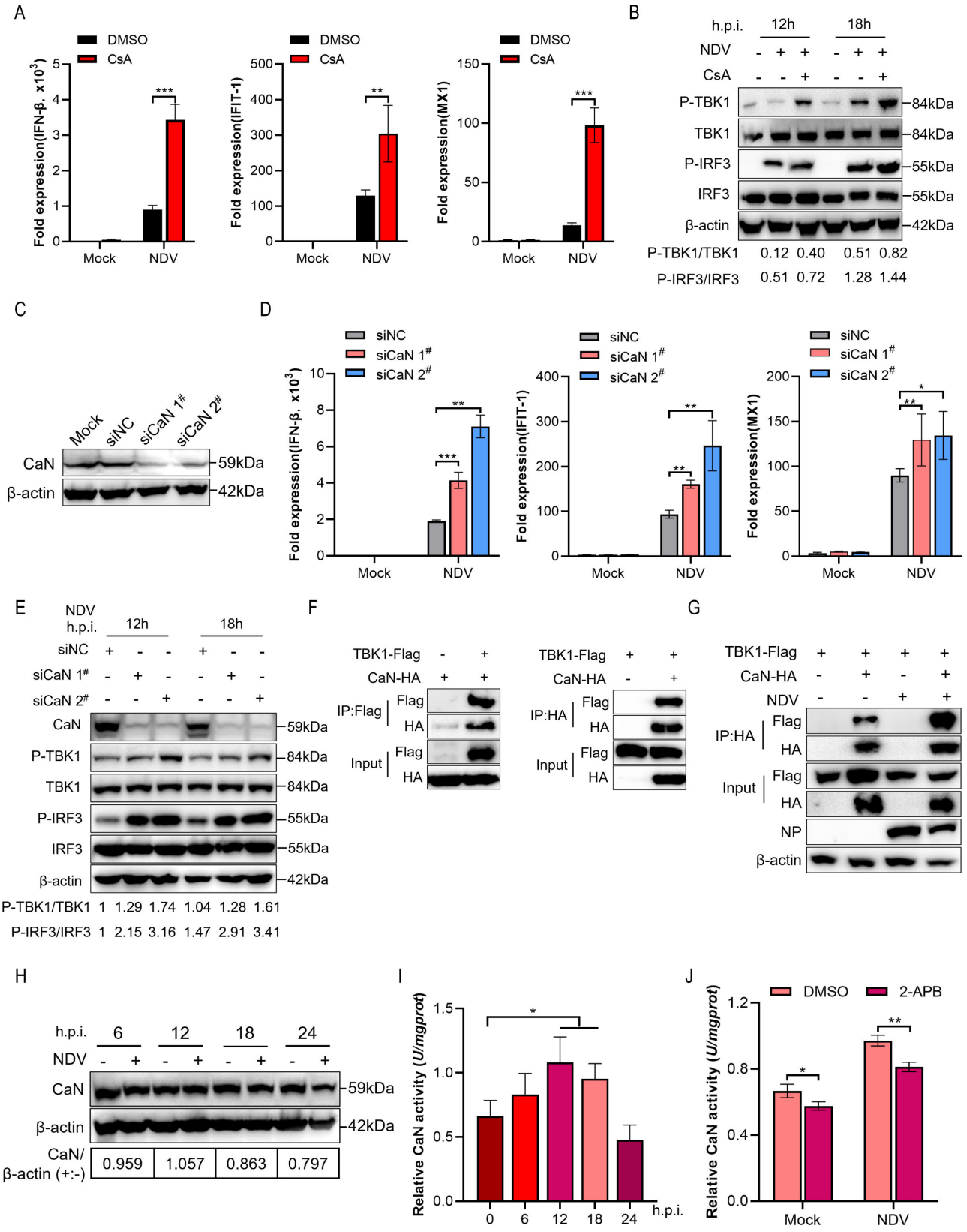

FIG 5 Calcineurin negatively regulates IFN-I signaling. (A) A549 cells were treated with or without CsA (10 μM), then mock treated or infected with NDV at an MOI of 1. At 12 h post-infection, cells were harvested, and qRT-PCR was used to detect IFN-β, IFIT-1, and MX1 mRNA expression levels. (B) Virus infection experiments were performed as described above for panel A. Cells were harvested at 12 and 18 h post-infection, and Western blot analysis was carried out to

(Continued on next page)

FIG 5 (Continued)

assess P-TBK1, TBK1, P-IRF3, and IRF3 protein expression levels. β-Actin acted as the loading control. (C) Cells were transfected with siRNA targeting CaN. Western blot analysis was used to determine the knockdown level of CaN. (D) A549 cells were transfected with CaN siRNA for 48 h, then infected with NDV at an MOI of 1. At 12 h post-infection, cells were harvested, and qRT-PCR was used to assess IFN-β , IFIT-1, and MX1 mRNA expression levels. (E) Virus infection experiments were performed as described above for panel D. Cells were harvested at 12 and 18 h post-infection, and Western blot analysis was used to detect P-TBK1, TBK1, P-IRF3, and IRF3 protein expression levels. β-Actin acted as the loading control. (F) HEK-293T cells were transfected with plasmids encoding Flag-TBK1 and HA-CaN for 24 h. Then, the supernatants of the cell lysates were immunoprecipitated using anti-Flag or anti-HA beads and immunoblotted with anti-HA or anti-Flag. (G) HEK-293T cells transfected with Flag-TBK1 and HA-CaN for 24 h were infected with NDV at an MOI of 1. Cells were harvested at 12 h post-infection, and the supernatants of the cell lysates were immunoprecipitated using anti-HA beads, then immunoblotted with anti-HA or anti-Flag. (H and I) A549 cells were infected with NDV at an MOI of 1. Cells were harvested at 0, 6, 12, 18, and 24 h post-infection, and Western blot analysis was carried out to determine CaN protein expression levels. β-Actin acted as the loading control (H). CaN activity was detected by spectrophotometry (I). (J) A549 cells were treated with or without 2-APB (100 μM), then mock treated or infected with NDV at an MOI of 1. At 18 h post-infection, cells were harvested and CaN activity was detected by spectrophotometry. Each bar represents the mean ± standard deviation. *$P < 0.05$, **$P < 0.01$, ***$P < 0.001$.

with the results that lack of extracellular Ca^{2+} had no positive effect on IFN-I production (Fig. 4G and H). Additionally, our findings revealed that the inhibition of CaN activity through CsA treatment (Fig. 7G and H) and CaN knockdown (Fig. 7I through K) on viral replication was counteracted in *TBK1*$^{-/-}$ cells. All these results clearly suggested that TBK1 is a key factor in Ca^{2+} signaling-mediated virus proliferation.

DISCUSSION

In-depth studies over the years have clearly shown that Ca^{2+} is an important component of the virus-host dialog (11, 41). Viruses exploit Ca^{2+} signaling networks to facilitate entry, replication, assembly, and export, as well as to establish persistent infection (12). In contrast, the host uses the accumulation of pathological Ca^{2+} signals to trigger cellular

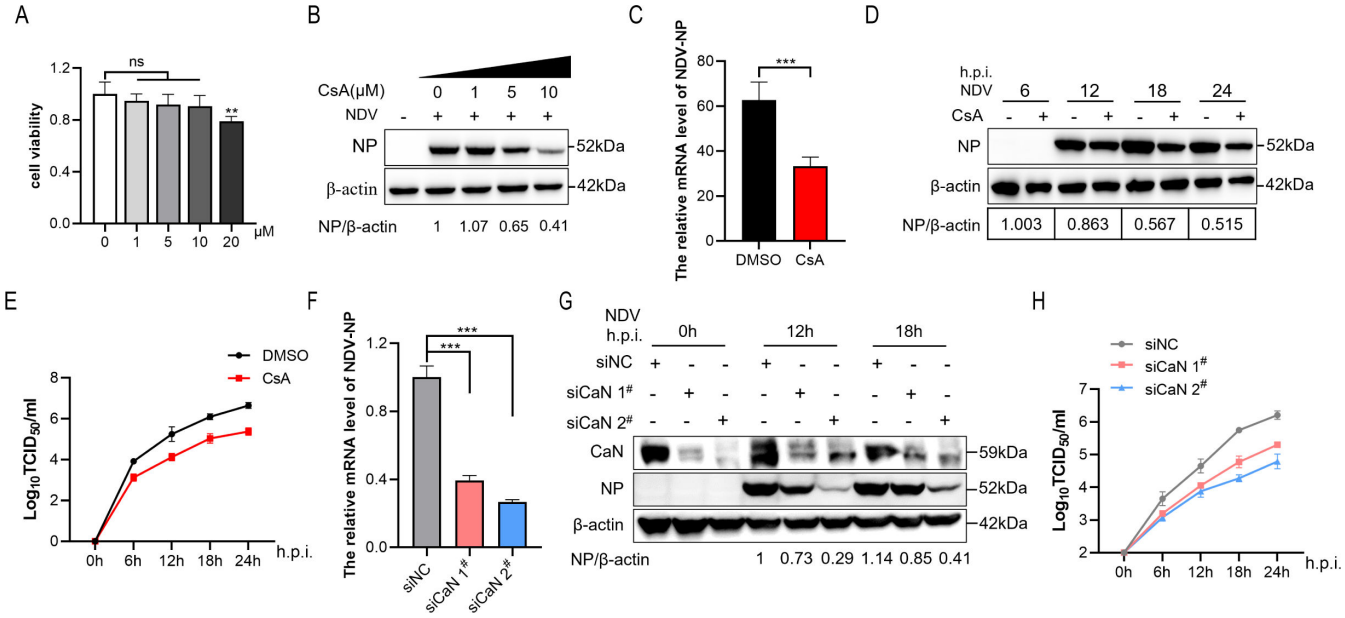

FIG 6 Inhibition of calcineurin activity inhibits virus replication. (A) A549 cells were spread on a 96-well plate for 24 h, and the effects of CsA on cell viability were detected by CCK-8. (B) A549 cells were treated with CsA (0, 1, 5, and 10 μM), then infected with NDV at an MOI of 1. Cells were harvested at 18 h post-infection, and NDV-NP expression levels were detected by Western blot analysis. β-Actin acted as the loading control. (C) A549 cells were treated with or without CsA (10 μM), then mock treated or infected with NDV at an MOI of 1. At 12 h post-infection, cells were harvested, and qRT-PCR was used to detect NDV-NP mRNA expression levels. (D and E) A549 cells were treated with or without CsA (10 μM) followed by infection with NDV (MOI of 1) for 0, 6, 12, 18, and 24 h. The amount of viral protein was quantified in the cell lysates (D), while cell culture supernatants were subjected to the viral titer assay (E). (F–H) A549 cells were transfected with CaN siRNA for 48 h, then infected with NDV at an MOI of 1. At 12 h post-infection, cells were harvested, and qRT-PCR was used to assess NDV-NP mRNA expression levels (F). At 12 or 18 h post-infection, NDV-NP expression levels were assessed by Western blotting (G). Cell culture supernatants were subjected to the viral titer assay (H). Each bar represents the mean ± standard deviation.**$P < 0.01$, ***$P < 0.001$.

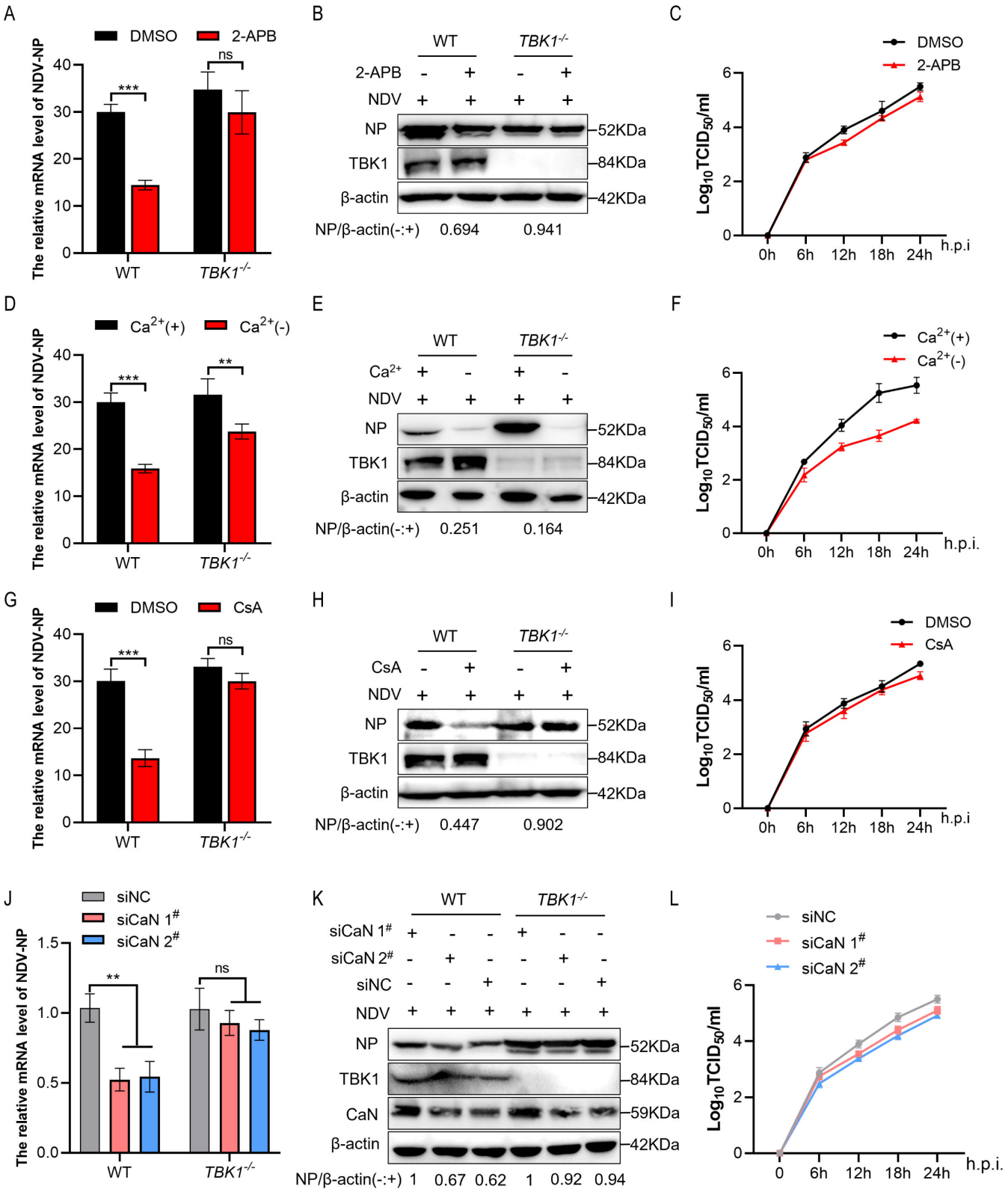

FIG 7 Knockout of *TBK1* inhibits the effect of Ca^{2+} and CaN on viral proliferation. (A–C) A549 cells were treated with or without 2-APB (100 µM), then mock treated or infected with NDV at an MOI of 1. The amounts of viral mRNA (A) and protein (B) and the viral titer assay (C). (D–F) A549 cells were cultured in normal medium or calcium-free medium followed by infection with NDV. The amounts of viral mRNA (D) and protein (E) and the viral titer assay (F). (G–I) A549 cells were treated with or without CsA (10 µM), then mock treated or infected with NDV at an MOI of 1. Cells were harvested, and qRT-PCR was used to detect NDV-NP

(Continued on next page)

FIG 7 (Continued)

mRNA expression levels. (G) The amount of viral mRNA and (H) protein and (I) the viral titer assay. (J–L) A549 cells were transfected with CaN siRNA for 48 h, then infected with NDV at an MOI of 1. (J) The amount of viral mRNA and (K) protein and (L) the viral titer assay. Each bar represents the mean ± standard deviation. ns >0.05, $^{**}P < 0.01$, $^{***}P < 0.001$.

immune responses or regulate other signaling networks to exert antiviral functions (17). Here, we have identified a previously unrecognized mechanism by which NDV infection escapes the host innate immune response by inducing an imbalance in Ca^{2+} homeostasis. In the present study, we found that NDV infection led to an increase in intracellular free Ca^{2+} and subsequent activation of CaN in a Ca^{2+}-dependent manner. Activated CaN then dephosphorylated TBK1 and inhibited IFN-I production. Thus, our findings indicate that increased Ca^{2+} suppresses TBK1 signaling and IFN-I expression, which may serve as an immune evasion pathway for NDV during infection.

In a resting state, the ER acts as the largest Ca^{2+} storage organelle within the cell, maintaining high intracellular Ca^{2+} levels and establishing concentration gradients with the cytoplasm and other organelles (42–44). Viruses take advantage of the large Ca^{2+} concentration in different organelles to regulate intracellular Ca^{2+} signaling by accelerating certain Ca^{2+}-dependent enzymatic processes and upregulating Ca^{2+}-sensitive transcription factors to create conditions conducive to their own replication (43). Our data demonstrated that intracellular Ca^{2+} depletion, either by Ca^{2+} withdrawal from the cell culture medium or by blocking the Ca^{2+} release from ER, successfully inhibited viral replication, suggesting that Ca^{2+} mobilization, including extracellular Ca^{2+} influx and intracellular Ca^{2+} release from the ER, is involved in regulating viral replication. Previous studies have reported that SeV and HSV-1 can trigger membrane perturbation-associated Ca^{2+} signaling and influx (45). Similarly, IAV has been shown to increase cytoplasmic Ca^{2+} release from the ER through increased activation of IP_3Rs or RyRs (46). These findings are consistent with our observations that both deletion of extracellular Ca^{2+} and inhibition of ER Ca^{2+} release inhibited viral replication. In addition, our findings revealed that virus-induced changes in intracellular Ca^{2+} homeostasis are adapted to viral replication. Further studies are required to determine the effects of such changes on viral proliferation.

2-APB and BAPTA-AM are widely used to prevent the increase of intracellular free Ca^{2+} during viral infection and have been implicated in the regulation of viral invasion, replication, maturation, and spread (47, 48). Although BAPTA-AM treatment inhibits the replication of many viruses (49, 50), in the current study, BAPTA-AM treatment did not inhibit NDV replication. However, inhibition of ER Ca^{2+} release by 2-APB or knockdown of IP_3R_1 and depletion of extracellular Ca^{2+} were found to inhibit NDV replication. Increased intracellular Ca^{2+} has been associated with the intense ER stress caused by NDV infection (38). ER stress can increase Ca^{2+} flux to promote viral replication (51), while BAPTA-AM can alleviate ER stress by chelating free Ca^{2+}. A moderate increase in intracellular Ca^{2+} induced by viral infection always seems to be beneficial for viral replication, and drugs that inhibit Ca^{2+} accumulation have different inhibitory effects on viral proliferation in different infection models (47), presumably due to the influence of different sources of Ca^{2+}. Regardless, the critical role played by Ca^{2+} during various stages of viral infection justifies the potential of Ca^{2+} as a target for antiviral therapy and the potential application of drugs that inhibit Ca^{2+} accumulation to antiviral therapy.

The mechanism by which replicating viruses trigger IFN-I induction through the generation and accumulation of viral pathogen-associated PRRs has been well characterized. Intracellular Ca^{2+} signaling is involved in regulating the activation of PRRs, promoting the activation of IFN regulatory factors, initiating the IFN-related innate immune response, and enhancing the NF-κB-associated inflammatory response (17). However, the involvement of Ca^{2+} in the regulation of innate immunity through PRRs is a large and complex network, and our understanding of PRR-mediated Ca^{2+} signaling-dependent cellular functions in different pathological processes remains limited. Furthermore, it is not fully understood how intracellular Ca^{2+} stimulates the activation of

PRR-related molecules. Here, we found that NDV-induced IFN-I production was activated in a Ca^{2+}-dependent manner following inhibition of ER Ca^{2+} release by 2-APB treatment but not after depletion of extracellular Ca^{2+}. These findings are not consistent with those reported in a recent study in which extracellular Ca^{2+} depletion was found to promote *Listeria monocytogenes*-induced IFN-β production (52). We speculate that the contradictory role may be due to different sources of Ca^{2+}. Based on our findings, we would predict that the vast majority of NDV-induced increases in intracellular Ca^{2+} originate from the ER, suggesting that ER Ca^{2+} release is more closely associated with IFN-I production. In addition, deficiencies in the Ca^{2+} sensor stromal interaction molecule 1 have been found to cause spontaneous activation of STING and enhanced expression of IFN-I, which is related to intracellular and extracellular Ca^{2+} flux (51). In summary, ER Ca^{2+} release is closely associated with extracellular Ca^{2+} influx, especially to balance the host innate immune response. Therefore, future studies should identify the source of increased intracellular pathological Ca^{2+} signaling caused by viral infection.

As a critical kinase in IFN-I signaling, TBK1 is activated by multiple adaptor proteins, including mitochondrial antiviral signaling protein and STING, and phosphorylates substrate transcription factors IRF3/IRF7 to initiate the antiviral innate immune response (2). Here, we found that inhibition of NDV-induced ER Ca^{2+} release dephosphorylated TBK1 and inhibited TBK1-mediated IFN-I production and antiviral immunity. CaN is a phosphatase involved in TBK1-mediated IFN-I production that is specifically activated by Ca^{2+} accumulated during viral infection (40). Our data suggest that NDV infection promotes dephosphorylation of TBK1 by CaN in a Ca^{2+}-dependent manner. In particular, we highlighted the critical role of TBK1 in Ca^{2+} signaling-mediated virus proliferation. However, since we did not examine whether CaN dephosphorylates other components of the IFN-I pathway, further studies are required to address this question. Interestingly, knockdown of CaN effectively inhibited NDV replication, although our data suggest an association with IFN-I. CaN has also been reported to bind to and dephosphorylate TFEB, thus promoting its nuclear translocation, which in turn promotes lysosomal biogenesis and autophagy (31). Since we have previously shown that autophagy favors NDV replication (53), further studies are required to determine whether CaN can also affect viral replication by regulating lysosomal biogenesis and autophagy. In addition, CsA, a CaN-specific inhibitor, has been widely used as an immunosuppressant to prevent the rejection of solid organ transplants and for the treatment of autoimmune diseases (54). Our results showed that treatment with CsA increased virus-induced IFN-I and inhibited viral replication, consistent with previous reports that CsA inhibited HCV (55) and HIV (56) replication. Together, these results suggest that CsA may also be suitable for the treatment of viral infectious diseases to inhibit viral proliferation and reduce the overactive inflammatory response.

In summary, we have identified a novel mechanism involving TBK1 through which NDV evades host antiviral immune responses. NDV induces intracellular Ca^{2+} accumulation, leading to activation of the serine/threonine phosphatase CaN and subsequent dephosphorylation of TBK1 and inhibition of IFN-I production and antiviral immunity (Fig. 8). We also found that Ca^{2+} depletion could effectively inhibit the proliferation of both RNA and DNA viruses and highlighted the potent antiviral effect of immunosuppressive agent CsA. Together, our findings will further the understanding of NDV immunosuppression, as well as provide a theoretical basis for antiviral therapy.

MATERIALS AND METHODS

Cells and viruses

A549, DF-1, HEK-293T, Vero, and BHK-21 cells were purchased from the American Type Culture Collection. Cells were maintained in Dulbecco's modified Eagle's medium (DMEM) supplemented with 10% fetal bovine serum (FBS) (Gibco, Franklin Lakes, NJ, USA). H1299 cells were purchased from the Cell Bank of Chinese Academy of Sciences and were maintained in Roswell Park Memorial Institute 1640 medium (Gibco) supplemented with

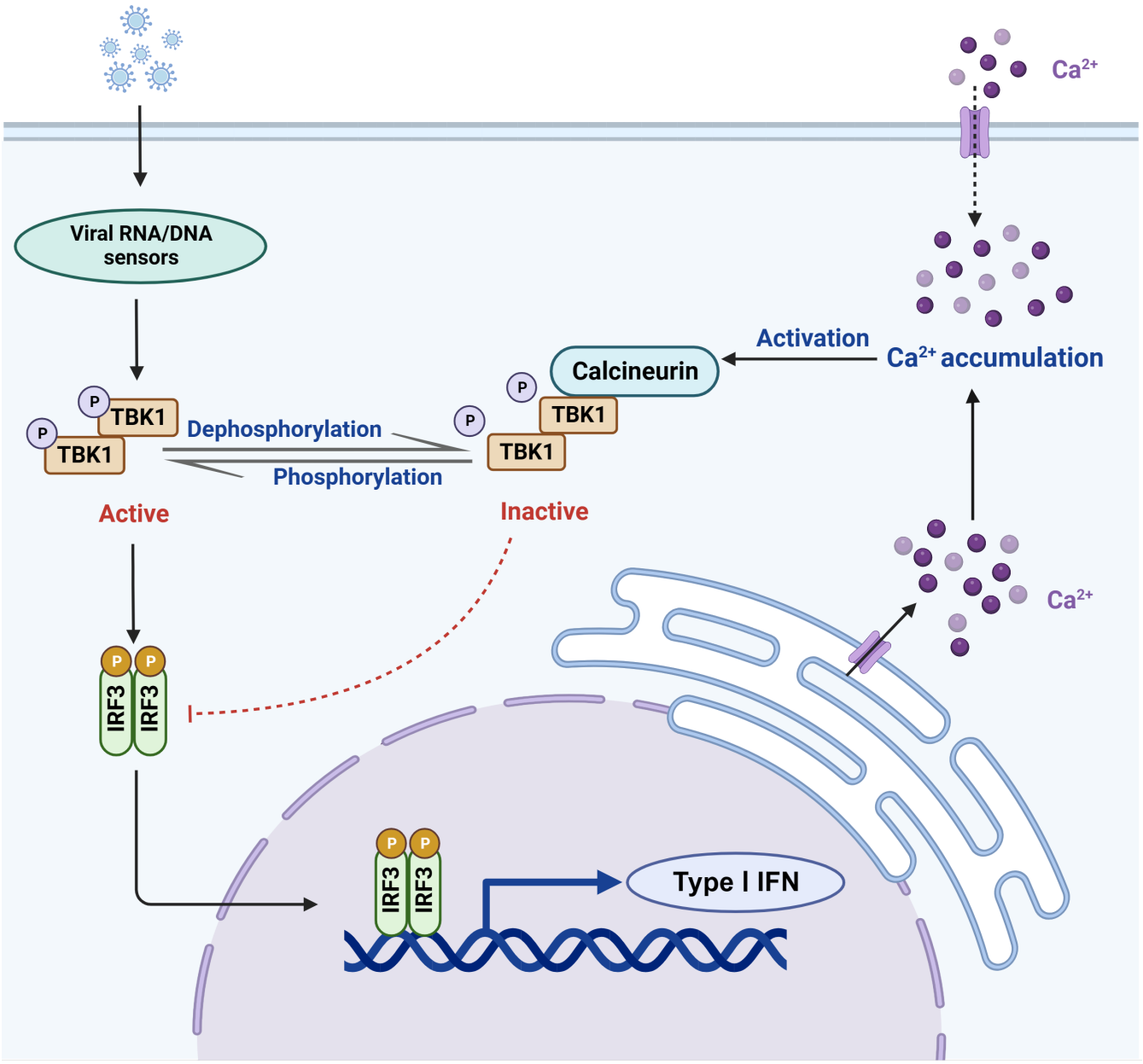

FIG 8 Model showing the negative regulation of IFN-I by the Ca^{2+}-calcineurin-TBK1 signaling pathway. NDV infection leads to the imbalance of intracellular Ca^{2+} homeostasis by inducing the accumulation of intracellular free Ca^{2+}, especially the release of Ca^{2+} from the ER, which promotes activation of CaN resulting in the dephosphorylation of TBK1 and inhibition of IFN-I, and finally replication of NDV.

10% FBS. *TBK1*$^{-/-}$ cells were provided by Qiyun Zhu (Lanzhou Veterinary Research Institute, China). CEF cells were prepared as previously described. The NDV Herts/33 strain was obtained from the China Institute of Veterinary Drug Control (Beijing, China). The NDV GFP-LaSota and RFP-LaSota strains were made and stored in our laboratory. SeV was provided by Quan Zhang (Yangzhou University, China). AIV was provided by Daxin Peng (Yangzhou University). VSV was provided by Jianchao Wei (Shanghai Veterinary Research Institute, China), and herpes simplex virus 1 (HSV-1) was provided by Yasushi Kawaguchi (University of Tokyo, Japan). NDV, AIV, VSV, and HSV-1 titers were determined as the median tissue culture infectious doses ($TCID_{50}$) in BHK-21 and Vero cells.

Antibodies and reagents

The IP_3R inhibitor 2-APB (T4693) was purchased from TopScience (Shanghai, China). The intracellular calcium chelator BAPTA-AM (HY-100545) and CaN phosphatase activity inhibitor CsA (HY-B0579) were purchased from MedChemExpress (Monmouth Junction, NJ, USA). Ca^{2+}-free DMEM was obtained from Gibco. $CaCl_2$ was purchased from Sigma-Aldrich (Merck KGaA, Darmstadt, Germany). Poly(I:C) was purchased from InvivoGen (San Diego, CA, USA). A monoclonal antibody against NDV-NP was prepared in our laboratory. A monoclonal antibody against avian influenza virus NP was provided by Daxin Peng (Yangzhou University). Rabbit polyclonal anti-Sendai virus (PD029C1) was purchased from MBL (Nagoya, Japan). Mouse monoclonal anti-VSV glycoprotein (ab50549) and rabbit monoclonal anti-calcineurin A (ab282104) were purchased from Abcam (Cambridge, MA, USA). Rabbit polyclonal anti-HSV-1 glycoprotein D (NB600-516) was purchased from Novus Biologicals (Littleton, CO, USA). Mouse monoclonal anti-Flag (F1804) was purchased from Sigma-Aldrich. Rabbit monoclonal anti-HA (3724), anti-IP_3R_1 (8568), anti-TBK1 (3013), anti-phospho-TBK1 (Ser172) (5483), anti-IRF3 (4302), and anti-phospho-IRF3 (Ser396) (4947) antibodies were purchased from Cell Signaling Technology (Beverly, MA, USA). Rabbit monoclonal anti-β-actin (AC006), goat anti-rabbit IgG (H + L) (AS014), and goat anti-mouse IgG (H + L) (AS003) antibodies were purchased from ABclonal (Wuhan, China). Alexa Fluor goat anti-rabbit-488 (A11034) and Alexa Fluor goat anti-rabbit-594 (A11037) antibodies were purchased from Invitrogen (Carlsbad, CA, USA).

Transfection of plasmids or siRNAs

HA-tagged CaN was constructed by inserting the open reading frame (ORF) of human *CaN* (GenBank accession no. NM_001130691.2) into the pCMV-HA plasmid (Promega). Flag-tagged TBK1 was constructed by inserting the ORF of human *TBK1* (GenBank accession no. NM_013254.4) into the p3XFLAG-CMV-14 plasmid (Sigma-Aldrich). All plasmid constructs were confirmed by DNA Sanger sequencing. siRNAs targeting endogenous *CaN* (siCaN 1#: 5′-CUCGUGUGGAUAUCUUAAATT-3′, siCaN 2#: 5′-GAGGGUACUUCAGUAUUGATT-3′) were purchased from GenePharma (Shanghai, China). Expression plasmids or siRNAs were transfected into HEK-293T or A549 cells using Lipofectamine 2000 (Thermo Fisher, USA) according to the manufacturer's instructions.

Cell viability assay

CCK-8 assays were used to determine cell viability. A549 cells were seeded in 96-well plates and treated with different concentrations of 2-APB, BAPTA-AM, CsA, or cultured in Ca^{2+}-free DMEM for 24 h. Subsequently, 10-µL CCK-8 solution (40203ES60; YEASEN, Shanghai, China) was added to each well. After 2-h incubation, the absorbance was measured at 450 nm using a microplate reader.

Measurement of intracellular Ca^{2+} levels

A549 cells were plated in six-well plates, pretreated with different reagents, and infected with NDV for the indicated time point. Cells were then incubated with the fluorescent Ca^{2+} indicator Fluo-4/AM (5 µM; AAT Bioquest, Pleasanton, USA) for 30 min in the dark. Samples were washed three times with phosphate-buffered saline (PBS), then immediately visualized directly by fluorescence microscopy at a wavelength of 488/525 nm (Olympus, Tokyo, Japan) or fluorescence intensity was measured by flow cytometry.

Virus titration

Viral titers were quantified by 50% $TCID_{50}$ or plaque assays. Briefly, DF-1 cells were seeded into 96- or 24-well plates. The virus-containing suspension was serially diluted 10-fold, then 100 or 300 µL/well was added to the 96- or 24-well plates, respectively, for 1 h at 37°C. Unbound virions were removed by washing with PBS. Maintenance medium

(DMEM containing 2% FBS) was added to the 96-well plates 3–5 days post-infection, and the $TCID_{50}$ was calculated using the Reed-Muench method. Cells seeded into 24-well plates were covered with medium containing methyl cellulose (1%) and cultured for 3–5 days. Cells were then fixed with 4% paraformaldehyde for 30 min at room temperature and stained with crystal violet solution for 30 min. Plaques were visualized and plaque-forming units were counted.

Quantitative real-time PCR

Total RNA was extracted from NDV-infected cells using the Cell/Tissue Total RNA Kit (19221ES50, YEASEN). Extracted RNA was reverse transcribed using One-Step gDNA Removal and cDNA Synthesis Super Mix (AE311; TransGen Biotech, Beijing, China) according to the manufacturer's instructions. Quantitative real-time PCR was carried out using universal blue qPCR SYBR Green Master Mix (11184ES08, YEASEN) and the following primers: human IFN-β, 5′-ACGACAGCTCTTTCCATGA-3′ (F) and 5′-AGCCAGTGCT CGATGAATCT-3′ (R); human IFIT-1, 5′-GCCATTTTCTTTGCTTCCCCT-3′ (F) and 5′-TGCCCTTT TGTAGCCTCCTTG-3′ (R); human β-actin, 5′-GATCTGGCACCACACCTTCT-3′ (F) and 5′-GGG GTGTTGAAGGTCTCAAA-3′ (R); human MX1, 5′-TGCGCCCCTGCATCGACCT-3′ (F) and 5′-GT TTCTTCAGTTTCAGCACCA-3′ (R); and NDV-NP, 5′-CAACAATAGGAGTGGAGTGTCTGA-3′ (F) and 5′- CAGGGTATCGGTGATGTCTTCT-3′(R). All experiments were carried out in triplicate.

Immunoblotting and coimmunoprecipitation

Harvested cells were lysed in 2× protein loading buffer (20-mM Tris-HCl, 2% SDS, 100-mM dithiothreitol, 20% glycerol, and 0.016% bromophenol blue), denatured, and resolved by 10% SDS-PAGE. Proteins were transferred to nitrocellulose membranes (NC-a101-b105; Whatman, Maidstone, UK). Each membrane was blocked in skim milk for 2 h at room temperature, incubated with primary antibodies overnight at 4°C, then washed three times with Tris-buffered saline with Tween 20 (TBS-T) [50-mM Tris-HCl (pH 7.6), 150-mM NaCl, and 0.1% Tween 20] for 10 min. Next, membranes were incubated with secondary antibodies for 2 h at room temperature and washed three times with TBS-T for 10 min. Protein bands were visualized using the Tanon 4600 Chemiluminescent Imaging System (Bio Tanon, Shanghai, China) and quantified using ImageJ software (National Institutes of Health, Bethesda, MD, USA). For coimmunoprecipitation, cells were transfected with expression vectors for 24 or 36 h, and total protein was extracted with RIPA lysis buffer (P0013D; Beyotime, Shanghai, China) containing 1-mM of the protease inhibitor phenylmethylsulfonyl (ST506, Beyotime). Lysates were centrifuged at 12,000 × *g* for 10 min and precipitated with anti-Flag or anti-HA-conjugated Dynabeads (ShareBio, Shanghai, China) overnight at 4°C. The beads were washed with lysis buffer three times, eluted with SDS loading buffer by boiling for 10 min, then subjected to immunoblotting.

Immunofluorescence assay

A549 cells were washed three times with PBS, fixed in 4% neutral formaldehyde for 30 min, then permeabilized with 0.5% Triton X-100 in TBS-T for 15 min. Samples were blocked with 3% bovine serum albumin for 45 min at room temperature, then incubated with primary antibodies for 2 h at 37°C or 4°C overnight, followed by incubation with secondary antibodies for 1 h at 37°C. Cells were washed again, and the nuclei were stained with 0.5-mg/mL 4′,6-diamidino-2-phenylindole. Between and after each incubation step, cells were washed three times with a blocking buffer. Finally, cells were visualized by confocal microscopy using a model LSM880 confocal microscope (Carl Zeiss, Jena, Germany). Images were analyzed using ImageJ software.

Calcineurin activity assay

Cells were infected with NDV and harvested at the corresponding time points. The CaN phosphatase activity was measured by the p-nitrophenyl phosphate (pNPP) method according to the manufacturer's instructions (KGT046, Keygen Biotech, Nanjing, China).

Statistical analysis

All data were analyzed using GraphPad Prism version 9.0 software (GraphPad Software, Inc.) and expressed as means ± standard deviations of at least three independent experiments. Significance was analyzed with two-tailed independent Student's *t*-tests between the two groups.

ACKNOWLEDGMENTS

We thank Quan Zhang (Yangzhou University, China) for providing the Sendai virus; Daxin Peng (Yangzhou University, China) for providing the avian influenza virus and the monoclonal antibody against the avian influenza virus nucleoprotein; Jianchao Wei (Shanghai Veterinary Research Institute, China) for providing the vesicular stomatitis virus; Yasushi Kawaguchi (University of Tokyo, Japan) for providing the herpes simplex virus-1; and Qiyun Zhu (Lanzhou Veterinary Research Institute, China) for providing tumor necrosis factor receptor-associated factor family member-associated NF-κB activator-binding kinase 1 cells.

This work was supported by the National Natural Science Foundation of China (32122085 and 32030108), the International Cooperation Project of National Natural Science Foundation of China (32220103012), and the National Key Research and Development Program of China (2022YFD1801500). The funders had no role in study design, data collection and analysis, decision to publish, or preparation of the article.

AUTHOR AFFILIATIONS

[1]College of Veterinary Medicine, Northwest A&F University, Yangling, Shaanxi, China
[2]Department of Avian Infectious Diseases, Shanghai Veterinary Research Institute, Chinese Academy of Agricultural Science, Shanghai, China
[3]College of Veterinary Medicine, South China Agricultural University, Guangzhou, China
[4]Jiangsu Co-innovation Center for Prevention and Control of Important Animal Infectious Diseases and Zoonoses, Yangzhou, China

AUTHOR ORCIDs

Yang Qu http://orcid.org/0009-0000-6928-7888
Xusheng Qiu http://orcid.org/0000-0001-6961-9774
Chan Ding http://orcid.org/0000-0003-0216-2129
Yingjie Sun http://orcid.org/0000-0002-6086-5722

FUNDING

Funder	Grant(s)	Author(s)
MOST | National Natural Science Foundation of China (NSFC)	32122085	Yingjie Sun
MOST | National Natural Science Foundation of China (NSFC)	32030108	Chan Ding
International Cooperation Project of National Natural Science Foundation of China	32220103012	Chan Ding
MOST | National Key Research and Development Program of China (NKPs)	2022YFD1801500	Yingjie Sun

AUTHOR CONTRIBUTIONS

Yang Qu, Data curation, Formal analysis, Writing – original draft | Siyuan Wang, Data curation, Validation | Hui Jiang, Data curation, Formal analysis | Qingyi Wang, Data curation | Ying Liao, Methodology, Project administration | Xusheng Qiu, Methodology | Lei Tan, Methodology | Cuiping Song, Methodology | Chan Ding, Conceptualization,

Funding acquisition, Project administration | Yingjie Sun, Funding acquisition, Methodology, Writing – review and editing | Zengqi Yang, Resources, Supervision

DATA AVAILABILITY

All data of this study are available from the corresponding author upon request, without undue reservation.

ADDITIONAL FILES

The following material is available online.

Supplemental Material

Supplemental figures (JVI0006-24-s0001.docx). Fig. S1 to S4.

REFERENCES

1. Bowie AG, Unterholzner L. 2008. Viral evasion and subversion of pattern-recognition receptor signalling. Nat Rev Immunol 8:911–922. https://doi.org/10.1038/nri2436
2. Fitzgerald KA, McWhirter SM, Faia KL, Rowe DC, Latz E, Golenbock DT, Coyle AJ, Liao SM, Maniatis T. 2003. IKKε and TBK1 are essential components of the IRF3 signaling pathway. Nat Immunol 4:491–496. https://doi.org/10.1038/ni921
3. Friedman CS, O'Donnell MA, Legarda-Addison D, Ng A, Cárdenas WB, Yount JS, Moran TM, Basler CF, Komuro A, Horvath CM, Xavier R, Ting AT. 2008. The tumour suppressor CYLD is a negative regulator of RIG-I-mediated antiviral response. EMBO Rep. 9:930–936. https://doi.org/10.1038/embor.2008.136
4. Lei CQ, Zhong B, Zhang Y, Zhang J, Wang S, Shu HB. 2010. Glycogen synthase kinase 3B regulates Irf3 transcription factor-mediated antiviral response via activation of the kinase Tbk1. Immunity 33:878–889. https://doi.org/10.1016/j.immuni.2010.11.021
5. Renner F, Saul VV, Pagenstecher A, Wittwer T, Schmitz ML. 2011. Inducible SUMO modification of TANK Alleviates its repression of Tlr7 signalling. EMBO Rep 12:129–135. https://doi.org/10.1038/embor.2010.207
6. Tang J, Yang Q, Xu C, Zhao H, Liu Y, Liu C, Zhou Y, Gai D, Pei R, Wang Y, Hu X, Zhong B, Wang Y, Chen X, Chen J. 2021. Histone deacetylase 3 promotes innate antiviral immunity through deacetylation of TBK1. Protein Cell 12:261–278. https://doi.org/10.1007/s13238-020-00751-5
7. Wang C, Chen T, Zhang J, Yang M, Li N, Xu X, Cao X. 2009. The E3 ubiquitin ligase Nrdp1 'preferentially' promotes TLR-mediated production of type I interferon. Nat Immunol 10:744–752. https://doi.org/10.1038/ni.1742
8. Berridge MJ, Bootman MD, Lipp P. 1998. Calcium - a life and death signal. Nature 395:645–648. https://doi.org/10.1038/27094
9. Kinoshita S, Su L, Amano M, Timmerman LA, Kaneshima H, Nolan GP. 1997. The T cell activation factor NF-ATc positively regulates HIV-1 replication and gene expression in T cells. Immunity 6:235–244. https://doi.org/10.1016/s1074-7613(00)80326-x
10. Rahman SK, Kerviel A, Mohl BP, He Y, Zhou ZH, Roy P. 2020. A calcium sensor discovered in bluetongue virus nonstructural protein 2 is critical for virus replication. J Virol 94:e01099-20. https://doi.org/10.1128/JVI.01099-20
11. Zhou Y, Frey TK, Yang JJ. 2009. Viral calciomics: interplays between Ca^{2+} and virus. Cell Calcium 46:1–17. https://doi.org/10.1016/j.ceca.2009.05.005
12. Qu Y, Sun Y, Yang Z, Ding C. 2022. Calcium ions signaling: targets for attack and utilization by viruses. Front Microbiol 13:889374. https://doi.org/10.3389/fmicb.2022.889374
13. Panda S, Behera S, Alam MF, Syed GH. 2021. Endoplasmic reticulum & mitochondrial calcium homeostasis: the interplay with viruses. Mitochondrion 58:227–242. https://doi.org/10.1016/j.mito.2021.03.008
14. Pinton P, Giorgi C, Siviero R, Zecchini E, Rizzuto R. 2008. Calcium and apoptosis: ER-mitochondria Ca^{2+} transfer in the control of apoptosis. Oncogene 27:6407–6418. https://doi.org/10.1038/onc.2008.308
15. Lahti AL, Manninen A, Saksela K. 2003. Regulation of T cell activation by HIV-1 accessory proteins: Vpr acts via distinct mechanisms to cooperate with Nef in NFAT-directed gene expression and to promote transactivation by CREB. Virology 310:190–196. https://doi.org/10.1016/s0042-6822(03)00164-8
16. Li YC, Boehning DF, Qian T, Popov VL, Weinman SA. 2007. Hepatitis C virus core protein increases mitochondrial ROS production by stimulation of ca uniporter activity . FASEB J 21:2474–2485. https://doi.org/10.1096/fj.06-7345com
17. Kong F, You H, Zheng K, Tang R, Zheng C. 2021. The crosstalk between pattern-recognition receptor signaling and calcium signaling. Int J Biol Macromol 192:745–756. https://doi.org/10.1016/j.ijbiomac.2021.10.014
18. Yamamura Y, Morizane S, Yamamoto T, Wada J, Iwatsuki K. 2018. High calcium enhances the expression of double-stranded RNA sensors and antiviral activity in epidermal keratinocytes. Exp Dermatol 27:129–134. https://doi.org/10.1111/exd.13456
19. Zhi X, Zhang Y, Sun S, Zhang Z, Dong H, Luo X, Wei Y, Lu Z, Dou Y, Wu R, Jiang Z, Weng C, Seong Seo H, Guo H. 2020. NLRP3 inflammasome activation by foot-and-mouth disease virus infection mainly induced by viral RNA and non-structural protein 2B. RNA Biol 17:335–349. https://doi.org/10.1080/15476286.2019.1700058
20. Nieto-Torres JL, Verdiá-Báguena C, Jimenez-Guardeño JM, Regla-Nava JA, Castaño-Rodriguez C, Fernandez-Delgado R, Torres J, Aguilella VM, Enjuanes L. 2015. Severe acute respiratory syndrome coronavirus E protein transports calcium ions and activates the NLRP3 inflammasome. Virology 485:330–339. https://doi.org/10.1016/j.virol.2015.08.010
21. Mathavarajah S, Salsman J, Dellaire G. 2019. An emerging role for calcium signalling in innate and autoimmunity via the cGAS-STING axis. Cytokine Growth Factor Rev 50:43–51. https://doi.org/10.1016/j.cytogfr.2019.04.003
22. Rusnak F, Mertz P. 2000. Calcineurin: form and function. Physiol Rev 80:1483–1521. https://doi.org/10.1152/physrev.2000.80.4.1483
23. Creamer TP. 2020. Calcineurin. Cell Commun Signal 18:137. https://doi.org/10.1186/s12964-020-00636-4
24. Li H, Rao A, Hogan PG. 2011. Interaction of calcineurin with substrates and targeting proteins. Trends Cell Biol 21:91–103. https://doi.org/10.1016/j.tcb.2010.09.011
25. Chin D, Means AR. 2000. Calmodulin: a prototypical calcium sensor. Trends Cell Biol 10:322–328. https://doi.org/10.1016/s0962--8924(00)01800-6
26. Swulius MT, Waxham MN. 2008. Ca^{2+}/calmodulin-dependent protein kinases. Cell Mol Life Sci 65:2637–2657. https://doi.org/10.1007/s00018-008-8086-2
27. Liu JO, Nacev BA, Xu J, Bhat S. 2009. It takes two binding sites for calcineurin and NFAT to tango. Mol Cell 33:676–678. https://doi.org/10.1016/j.molcel.2009.03.005
28. Kraner SD, Norris CM. 2018. Astrocyte activation and the calcineurin/NFAT pathway in cerebrovascular disease. Front Aging Neurosci 10:287. https://doi.org/10.3389/fnagi.2018.00287

29. Tremblay ML, Giguère V. 2008. Phosphatases at the heart of FoxO metabolic control. Cell Metab 7:101–103. https://doi.org/10.1016/j.cmet.2008.01.004
30. Parra V, Rothermel BA. 2017. Calcineurin signaling in the heart: the importance of time and place. J Mol Cell Cardiol 103:121–136. https://doi.org/10.1016/j.yjmcc.2016.12.006
31. Medina DL, Ballabio A. 2015. Lysosomal calcium regulates autophagy. Autophagy 11:970–971. https://doi.org/10.1080/15548627.2015.1047130
32. Hendus-Altenburger R, Wang X, Sjøgaard-Frich LM, Pedraz-Cuesta E, Sheftic SR, Bendsøe AH, Page R, Kragelund BB, Pedersen SF, Peti W. 2019. Molecular basis for the binding and selective dephosphorylation of Na^+/H^+ exchanger 1 by calcineurin. Nat Commun 10:3489. https://doi.org/10.1038/s41467-019-11391-7
33. Woolfrey KM, Dell'Acqua ML. 2015. Coordination of protein phosphorylation and dephosphorylation in synaptic plasticity. J Biol Chem 290:28604–28612. https://doi.org/10.1074/jbc.R115.657262
34. Tokheim AM, Martin BL. 2006. Association of calcineurin with mitochondrial proteins. Proteins 64:28–33. https://doi.org/10.1002/prot.20996
35. Pennanen C, Parra V, López-Crisosto C, Morales PE, Del Campo A, Gutierrez T, Rivera-Mejías P, Kuzmicic J, Chiong M, Zorzano A, Rothermel BA, Lavandero S. 2014. Mitochondrial fission is required for cardiomyocyte hypertrophy mediated by a Ca-calcineurin signaling pathway. J Cell Sci 127:2659–2671. https://doi.org/10.1242/jcs.139394
36. Bendickova K, Tidu F, Fric J. 2017. Calcineurin-NFAT signalling in myeloid leucocytes: new prospects and pitfalls in immunosuppressive therapy. EMBO Mol Med 9:990–999. https://doi.org/10.15252/emmm.201707698
37. Ganar K, Das M, Sinha S, Kumar S. 2014. Newcastle disease virus: current status and our understanding. Virus Res 184:71–81. https://doi.org/10.1016/j.virusres.2014.02.016
38. Li YR, Jiang WY, Niu QN, Sun YJ, Meng CC, Tan L, Song CP, Qiu XS, Liao Y, Ding C. 2019. eIF2α-CHOP-BCl-2/JNK and IRE1α-XBP1/JNK signaling promote apoptosis and inflammation and support the proliferation of Newcastle disease virus. Cell Death Dis 10:891. https://doi.org/10.1038/s41419-019-2128-6
39. Ren SH, Rehman ZU, Shi MY, Yang B, Liu PR, Yin YC, Qu YR, Meng CC, Yang ZQ, Gao XL, Sun YJ, Ding C. 2019. Hemagglutinin-neuraminidase and fusion proteins of virulent Newcastle disease virus cooperatively disturb fusion-fission homeostasis to enhance mitochondrial function by activating the unfolded protein response of endoplasmic reticulum and mitochondrial stress. Vet Res 50:37. https://doi.org/10.1186/s13567-019-0654-y
40. Huang HJ, Xiong QQ, Wang N, Chen RY, Ren H, Siwko S, Han HH, Liu MY, Qian M, Du B. 2018. Kisspeptin/GPR54 signaling restricts antiviral innate immune response through regulating calcineurin phosphatase activity. Sci Adv 4:eaas9784. https://doi.org/10.1126/sciadv.aas9784
41. Chen XJ, Cao RY, Zhong W. 2020. Host calcium channels and pumps in viral infections. Cells 9:94. https://doi.org/10.3390/cells9010094
42. Berridge MJ, Bootman MD, Roderick HL. 2003. Calcium signalling: dynamics, homeostasis and remodelling. Nat Rev Mol Cell Biol 4:517–529. https://doi.org/10.1038/nrm1155
43. Raffaello A, Mammucari C, Gherardi G, Rizzuto R. 2016. Calcium at the center of cell signaling: interplay between endoplasmic reticulum, mitochondria, and lysosomes. Trends Biochem Sci 41:1035–1049. https://doi.org/10.1016/j.tibs.2016.09.001
44. Zampese E, Pizzo P. 2012. Intracellular organelles in the saga of Ca^{2+} homeostasis: different molecules for different purposes? Cell Mol Life Sci 69:1077–1104. https://doi.org/10.1007/s00018-011-0845-9
45. Hare DN, Collins SE, Mukherjee S, Loo YM, Gale M, Janssen LJ, Mossman KL. 2015. Membrane perturbation-associated Ca^{2+} signaling and incoming genome sensing are required for the host response to low-level enveloped virus particle entry. J Virol 90:3018–3027. https://doi.org/10.1128/JVI.02642-15
46. Hartshorn KL, Collamer M, Auerbach M, Myers JB, Pavlotsky N, Tauber AI. 1988. Effects of influenza A virus on human neutrophil calcium metabolism. J Immunol 141:1295–1301.
47. Kumar PS, Radhakrishnan A, Mukherjee T, Khamaru S, Chattopadhyay S, Chattopadhyay S. 2023. Understanding the role of Ca via transient receptor potential (TRP) channel in viral infection: implications in developing future antiviral strategies. Virus Res. 323:198992. https://doi.org/10.1016/j.virusres.2022.198992
48. Wang SB, Liu Y, Guo J, Wang PL, Zhang LK, Xiao GF, Wang W. 2017. Screening of FDA-approved drugs for inhibitors of Japanese encephalitis virus infection. J Virol 91. https://doi.org/10.1128/JVI.01055-17
49. Dellis O, Arbabian A, Papp B, Rowe M, Joab I, Chomienne C. 2011. Epstein-Barr virus latent membrane protein 1 increases calcium influx through store-operated channels in B lymphoid cells. J Biol Chem 286:18583–18592. https://doi.org/10.1074/jbc.M111.222257
50. Groppelli E, Starling S, Jolly C. 2015. Contact-induced mitochondrial polarization supports HIV-1 virological synapse formation. J Virol 89:14–24. https://doi.org/10.1128/JVI.02425-14
51. Diao FF, Jiang CL, Sun YY, Gao YN, Bai J, Nauwynck H, Wang XW, Yang YQ, Jiang P, Liu X. 2023. Porcine reproductive and respiratory syndrome virus infection triggers autophagy via ER stress-induced calcium signaling to facilitate virus replication. PLoS Pathog. 19:e1011295. https://doi.org/10.1371/journal.ppat.1011295
52. Kwon D, Sesaki H, Kang SJ. 2018. Intracellular calcium is a rheostat for the STING signaling pathway. Biochem Biophys Res Commun 500:497–503. https://doi.org/10.1016/j.bbrc.2018.04.117
53. Sun YJ, Yu SQ, Ding N, Meng CC, Meng SS, Zhang SL, Zhan Y, Qiu XS, Tan L, Chen HJ, Song CP, Ding C. 2014. Autophagy benefits the replication of Newcastle disease virus in chicken cells and tissues. J Virol 88:525–537. https://doi.org/10.1128/JVI.01849-13
54. Beauchesne PR, Chung NSC, Wasan KM. 2007. Cyclosporine A: a review of current oral and intravenous delivery systems. Drug Dev Ind Pharm 33:211–220. https://doi.org/10.1080/03639040601155665
55. Firpi RJ, Zhu H, Morelli G, Abdelmalek MF, Soldevila-Pico C, Machicao VI, Cabrera R, Reed AI, Liu C, Nelson DR. 2006. Cyclosporine suppresses hepatitis C virus *in vitro* and increases the chance of a sustained virological response after liver transplantation. Liver Transpl 12:51–57. https://doi.org/10.1002/lt.20532
56. Wainberg MA, Dascal A, Blain N, Fitz-Gibbon L, Boulerice F, Numazaki K, Tremblay M. 1988. The effect of cyclosporine A on infection of susceptible cells by human immunodeficiency virus type 1. Blood 72:1904–1910. https://doi.org/10.1182/blood.V72.6.1904.1904